1521-0111/12/8206-1094–1103$25.00
MOLECULAR PHARMACOLOGY
Vol. 82, No. 6
80275/3804879

Mol Pharmacol 82:1094–1103, 2012

Identification of Structural Motifs Critical for Epstein-Barr Virus-Induced Molecule 2 Function and Homology Modeling of the Ligand Docking Site[S]

Li Zhang, Amy Y. Shih, Xia V. Yang,[1] Chester Kuei, Jiejun Wu, Xiaohu Deng, Neelakandha S. Mani, Taraneh Mirzadegan, Siquan Sun, Timothy W. Lovenberg, and Changlu Liu

Janssen Pharmaceutical Research and Development, San Diego, California

Received June 1, 2012; accepted August 28, 2012

ABSTRACT

Epstein-Barr virus-induced molecule 2 (EBI2) (also known as G-protein–coupled receptor 183) is a G-protein–coupled receptor (GPCR) that is best known for its role in B cell migration and localization. Our recent deorphanization effort led to the discovery of 7α,25-dihydroxycholesterol (7α,25-OHC) as the endogenous ligand for EBI2, which provides a tool for mechanistic studies of EBI2 function. Because EBI2 is the first GPCR known to bind and to be activated by an oxysterol, the goal of this study was to understand the molecular and structural bases for its ligand-dependent activation; this was achieved by identifying structural moieties in EBI2 or in 7α,25-OHC that might affect receptor-ligand interactions. By using a series of chemically related OHC analogs, we demonstrated that all three hydroxyl groups in 7α,25-OHC contributed to ligand-induced activation of the receptor. To determine the location and composition of the ligand binding domain in EBI2, we used a site-directed mutagenesis approach and generated mutant receptors with single amino acid substitutions at selected positions of interest. Biochemical and pharmacological profiling of these mutant receptors allowed for structure-function analyses and revealed critical motifs that likely interact with 7α,25-OHC. By using a hybrid β_2-adrenergic receptor–C-X-C chemokine receptor type 4 structure as a template, we created a homology model for EBI2 and optimized the docking of 7α,25-OHC into the putative ligand binding site, so that the hydroxyl groups interact with residues Arg87, Asn114, and Glu183. This model of ligand docking yields important structural insight into the molecular mechanisms mediating EBI2 function and may facilitate future efforts to design novel therapeutic agents that target EBI2.

Introduction

Epstein-Barr virus-induced molecule 2 (EBI2), also known as GPR183, is a GPCR that was originally identified as a gene that is highly up-regulated upon Epstein-Barr virus infection (Birkenbach et al., 1993). EBI2 is expressed most abundantly in lymphoid tissues, such as spleen and lymph nodes (Birkenbach et al., 1993; Rosenkilde et al., 2006). Although it is classified as a class A rhodopsin-like GPCR (Vassilatis et al., 2003), EBI2 lacks strong sequence similarity to most other GPCRs. The closest homolog is GPR18, which exhibits 52% similarity to EBI2 (Benned-Jensen and Rosenkilde, 2008). Previous studies showed that EBI2 signals through $G\alpha_i$ but not $G\alpha_s$ or $G\alpha_q$ (Rosenkilde et al., 2006; Hannedouche et al., 2011; Liu et al., 2011). Activation of EBI2 leads to adenylate cyclase inhibition and subsequent reduction of cAMP production. EBI2 also was reported to activate extracellular signal-regulated kinase (Benned-Jensen et al., 2011).

Significant progress has been made in determining the functional significance of EBI2 in the immune system (Gatto et al., 2009, 2011; Pereira et al., 2009, 2010; Hannedouche et al., 2011; Kelly et al., 2011; Liu et al., 2011). It is now widely acknowledged that EBI2 expression and EBI2-mediated chemotaxis represent important molecular mechanisms for directing follicular B cell migration and localization. Up-regulation of EBI2 expression in B cells during early stages of an immune response promotes the movement of activated B cells to the outer follicle and interfollicular regions, whereas

[1] Current affiliation: Regulus Therapeutics, San Diego, California.

Article, publication date, and citation information can be found at http://molpharm.aspetjournals.org.
http://dx.doi.org/10.1124/mol.112.080275.

[S] The online version of this article (available at http://molpharm.aspetjournals.org) contains supplemental material.

ABBREVIATIONS: EBI2, Epstein-Barr virus-induced molecule 2; CXCR, C-X-C chemokine receptor; β_2AR, β_2-adrenergic receptor; ECL, extracellular loop; GPCR, G-protein–coupled receptor; GTPγS, guanosine 5′-*O*-(3-thio)triphosphate; OHC, hydroxycholesterol; PDB, Protein Data Bank; TM, transmembrane region; GPR, G-protein–coupled receptor.

down-regulation of EBI2 expression allows B cells to move to the center of follicles for germinal center formation. These carefully orchestrated events are part of an intricate, well-balanced network of chemokine receptors that includes EBI2, CXCR5, C-C chemokine receptor type 7, and CXCR4 (Gatto et al., 2011; Kelly et al., 2011). Together, they are responsible for providing B cells with a precise plan for mounting correct antibody responses when necessary. B cells from EBI2-deficient mice were reported to exhibit abnormal migration patterns and reduced antibody responses (Liu et al., 2011).

We identified an oxysterol, 7α,25-OHC, as the most likely endogenous ligand for EBI2 (Liu et al., 2011). 7α,25-OHC (structure shown in Fig. 2A) is an oxygenated derivative of cholesterol and is converted endogenously from 25-OHC by the enzyme CYP7B1 (Rose et al., 1997). 7α,25-OHC binds EBI2 with a dissociation constant of 450 pM and activates EBI2 with an EC_{50} of 140 pM, which makes it more potent than the other oxysterols we tested. Functionally, 7α,25-OHC directs B cell migration both in vitro and in vivo. Pharmacological blockade of 7α,25-OHC synthesis disrupts B cell migration patterns, consistent with findings observed with B cells from EBI2-deficient mice (Liu et al., 2011). Similar results were reported by Hannedouche et al. (2011).

Identification of 7α,25-OHC as the endogenous ligand for EBI2 revealed an important link between EBI2 and its known function in the immune system and allowed us to measure receptor activation quantitatively in vitro. Previous structure-function studies with EBI2 were focused largely on investigating its constitutive activity. Those studies revealed important structural motifs for the ligand-independent activity of the receptor and suggested potential molecular constraints during receptor transition from the inactive conformation to the active conformation (Benned-Jensen and Rosenkilde, 2008; Benned-Jensen et al., 2011). We decided to explore the molecular mechanisms of ligand-dependent activation of EBI2 by using 7α,25-OHC as a tool. We showed previously that the hydroxyl groups in the 7′- and 25′-positions of 7α,25-OHC are important for ligand activity (Liu et al., 2011). Here we demonstrate that the 3′-hydroxyl group, which is native to the steroidal body of cholesterol, is also a critical component of receptor-ligand interactions. To distinguish the structural motifs in EBI2 that are important for receptor activity, we used a mutagenesis approach and made single amino acid changes at various positions in the receptor, the majority of which were side-chain eliminations with Ala substitutions. Transmembrane region mutations were proposed on the basis of sequence alignment of EBI2 with GPCRs with known X-ray crystal structures. Mutations in the extracellular loops were proposed mainly on the basis of conservation among different species (Fig. 1). By measuring receptor expression, receptor activation, and radioligand binding, we characterized the pharmacological profiles of mutant receptors and identified key residues mediating receptor function. These structure-activity data were incorporated into a homology model of EBI2. By using a hybrid β_2AR-CXCR4 structure as a template, we were able to dock 7α,25-OHC and to define the putative ligand binding site. This information may facilitate the rational design of small-molecule compounds to serve as agonists or antagonists of EBI2.

Materials and Methods

Materials. Unless indicated otherwise, all materials were purchased from Sigma-Aldrich (St. Louis, MO). 7α,25-OHC, 7α,27-OHC, and 7α,27-dihydroxy-4-cholesten-3-one were purchased from Avanti Polar Lipids (Alabaster, AL). ^{3}H-labeled 7α,25-OHC (specific activity, 30 Ci/mmol) was custom-synthesized by Moravek Biochemicals (Brea, CA). Cell culture reagents were purchased from Thermo Fisher Scientific (Waltham, MA). Lipofectamine transfection reagent and anti-V5 mouse monoclonal antibody were purchased from Invitrogen (Carlsbad, CA).

Site-Directed Mutagenesis of EBI2. The coding region of human *ebi2* (GenBank accession no. NM_004951.4) with a V5 tag at the N terminus (V5-*ebi2*) was cloned into the mammalian expression vector pCIneo, as described (Liu et al., 2011). For site-directed mutagenesis, wild-type V5-*ebi2* served as a template for polymerase chain reaction amplifications with primers that contained the mutated sequence. The mutated *ebi2* DNA was inserted back into the pCIneo vector, and all constructs were verified through DNA sequencing at Eton Bioscience (San Diego, CA). A complete list of mutations is presented in Supplemental Table 1.

Tissue Culture and Recombinant Expression of Mutant Human EBI2. COS-7 cells were grown in Dulbecco's modified Eagle's medium (Invitrogen; with 4500 mg/liter glucose, 10% fetal bovine serum, 1% penicillin-streptomycin, 1 mM sodium pyruvate, and 20 mM HEPES) at 5% CO_2 and 37°C. Transient transfections of COS-7 cells were performed by using Lipofectamine reagent in Opti-MEM (Invitrogen), according to the manufacturer's instructions. For receptor expression characterization, cells were transiently transfected with V5-tagged *ebi2* alone. For GTPγS and radioligand binding assays, cells were cotransfected with *ebi2* constructs plus a human G-protein (G_{o2}) expression construct that contained the coding region of human G_{o2} (GenBank accession no. AF493895) in the mammalian expression vector pcDNA3.1/zeo. The transfected cells were harvested 48 h later, and cell pellets were stored at −80°C until GTPγS and radioligand binding assays were performed.

Characterization of Receptor Expression. For assessment of total and cell-surface receptor expression levels, transiently transfected cells were seeded in 96-well culture plates, in triplicate (4×10^4 cells/well), 24 h after transfection. Cells were fixed with 4% paraformaldehyde 2 days after transfection. Total and cell-surface expression levels for V5-tagged receptor proteins were quantified with enzyme-linked immunosorbent assays with an anti-V5 antibody (1 μg/ml), in the presence of 1% Triton X-100 (for total protein levels) or in the absence of Triton X-100 (for cell-surface protein levels). Cells transfected with the G_{o2} expression construct alone were used as negative controls. Cells transfected with the wild-type V5-ebi2 construct were used as positive controls. Cells transfected with GPR81-V5, a GPR81 expression construct with a V5 tag at the C terminus, were also included as controls.

GTPγS Binding Assays. [^{35}S]GTPγS binding assays were performed as described (Liu et al., 2003). Membrane preparations from transfected cells were added to 96-well plates and were incubated with different concentrations of ligand at room temperature for 20 min. [^{35}S]GTPγS (PerkinElmer Life and Analytical Sciences, Waltham, MA) was then added to the mixture at a final concentration of 200 pM. The reactions were allowed to proceed at room temperature for 1 h, and the reaction mixtures were filtered though a 96-well GFC filter plate (PerkinElmer Life and Analytical Sciences) and washed with buffer (20 mM Tris-HCl, 10 mM $MgCl_2$, pH 7.4); 50 μl of Microscint-40 (PerkinElmer Life Sciences) was added to each well, and the plate was assessed with a TopCount NXT counter (PerkinElmer Life and Analytical Sciences). Assays were performed in triplicate, and results were analyzed with GraphPad Prism 5 (GraphPad Software Inc., San Diego, CA). Values for [^{35}S]GTPγS incorporation in the presence of ligand activation were normalized as percentage increases over basal levels measured in the absence of ligands. EC_{50} values were calculated as the ligand concentrations

A

```
Human:     MANNFTPPSATPQGNDCDLYAHHSTARIVMPLHYSLVFIIGLVGNLLALVVIVQNRKKIN  64
Rat:       MANNFTTPLAASHGNNCDLYAHHSTARILMPLHYSLVFIIGLVGNLLALVVIVQNRKKIN  60
Mouse:     MANNFTTPLATSHGNNCDLYAHHSTARVLMPLHYSLVFIIGLVGNLLALVVIVQNRKKIN  60
Consensus: MANNFT-P-A---GN+CDLYAHHSTARI+MPLHYSLVFIIGLVGNLLALVVIVQNRKKIN
                                          TM1
Human:     STTLYSTNLVISDILFTTALPTRIAYYAMGFDWRIGDALCRITALVFYINTYAGVNFMTC  124
Rat:       STTLYSMNLVISDILFTTALPTRIVYYALGFDWRIGDALCRITALLFYINTYAGVNFMTC  120
Mouse:     STTLYSMNLVISDILFTTALPTRIAYYALGFDWRIGDALCRVTALVFYINTYAGVNFMTC  120
Consensus: STTLYS-NLVISDILFTTALPTRI-YYA+GFDWRIGDALCRITAL+FYINTYAGVNFMTC
                      TM2                                  TM3
Human:     LSIDRFIAVVHPLRYNKIKRIEHAKGVCIFVWILVFAQTLPLLINPMSKQEAERITCMEY  184
Rat:       LSIDRFFAVVHPLRYNKIKRIEYAKGICVFVWILVFAQTLPLLLKPMSKQEADKTTCMEY  180
Mouse:     LSIDRFFAVVHPLRYNKIKRIEYAKGVCLSVWILVFAQTLPLLLTPMSKEEGDKTTCMEY  180
Consensus: LSIDRF-AVVHPLRYNKIKRIE+AKG+C+FVWILVFAQTLPLL+-PMSKQEA++-TCMEY
                                          TM4
Human:     PNFEETKSLPWILLGACFIGYVLPLIIILICYSQICCKLFRTAKQNPLTEKSGVNKKALN  244
Rat:       PNFEGTASLPWILLGACLLGYVLPLAIILLCYSQICCKLFRTAKQNPLTEKSGVNKKALN  240
Mouse:     PNFEGTASLPWILLGACLLGYVLPITVILLCYSQICCKLFRTAKQNPLTEKSGVNKKALN  240
Consensus: PNFE-T-SLPWILLGAC-+GYVLPL-IIL+CYSQICCKLFRTAKQNPLTEKSGVNKKALN
                      TM5
Human:     TIILIIVVFVLCFTPYHVAIIQHMIKKLRFSNFLECSQRHSFQISLHFTVCLMNFNCCMD  304
Rat:       TIILIIGVFVLCFTPYHVAIMQHMVKTLYAPGALGCGVRHSFQISLHFTVCLMNFNCCMD  300
Mouse:     TIILIIVVFILCFTPYHVAIIQHMIKMLCSPGALECGARHSFQISLHFTVCLMNFNCCMD  300
Consensus: TIILII-VFVLCFTPYHVAI+QHM+K-L-----L-C--RHSFQISLHFTVCLMNFNCCMD
                TM6                                        TM7
Human:     PFIYFFACKGYKRKVMRMLKRQVSVSISSAVKSAPEENSREMTETQMMIHSKSSNGK  361
Rat:       PFIYFFACKGYKRKVMKMLKRQVSVSISSAVRSAPEENSREMTESQMMIHSKASNGR  357
Mouse:     PFIYFFACKGYKRKVMKMLKRQVSVSISSAVRSAPEENSREMTESQMMIHSKASNGR  357
Consensus: PFIYFFACKGYKRKVM+MLKRQVSVSISSAV+SAPEENSREMTE+QMMIHSK+SNG+  357
```

B

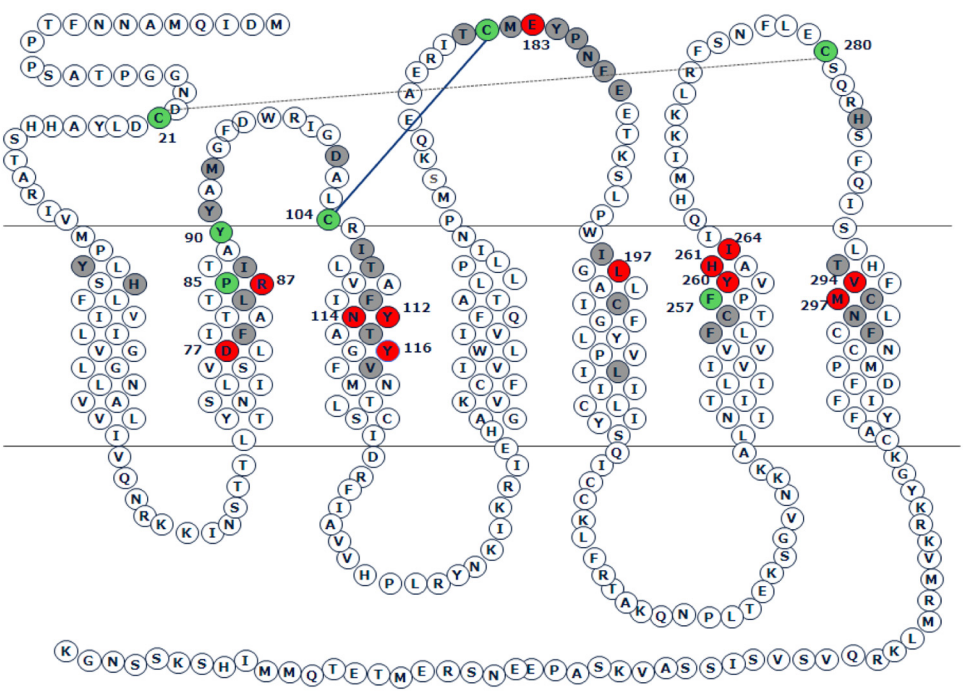

Fig. 1. A, amino acid sequence comparison of human, rat, and mouse EBI2 sequences. Underlined sequences, transmembrane regions. B, diagram showing amino acid sequence and predicted transmembrane regions of human EBI2. Residues shown in color (gray, green, and red) are the positions where mutations were introduced. Residues shown in red were found to be important for receptor ligand binding or receptor activation. Residues shown in green, including the four Cys residues in the extracellular region, affected receptor expression when mutated to Ala. Residues shown in gray had little or no effect on the pharmacological characteristics of the receptor. Solid line, classic disulfide bond between Cys104 and Cys181. Dashed line, potential second disulfide bridge between Cys21 and Cys280.

that stimulated 50% of the maximal response (E_{max}). The maximal response of wild-type EBI2 to 7α,25-OHC was expressed as 100% and was used for comparisons of maximal GTPγS incorporation for all mutant receptors. EC_{50} and E_{max} values were not calculated for mutants that did not reach a plateau in GTPγS binding assays at the highest concentration of ligand used (1 μM for 7α,25-OHC and 10 μM for 7α,27-dihydroxy-4-cholesten-3-one).

Radioligand Binding Assays. [^{3}H]7α,25-OHC was used in competition binding experiments as described previously (Liu et al., 2001, 2011). Membrane preparations from COS-7 cells transiently expressing wild-type or mutant EBI2 were incubated with [^{3}H]7α,25-OHC (100,000 cpm) in the presence of various concentrations of unlabeled 7α,25-OHC as a competitor. We used unlabeled 7α,25-OHC as the competitor because it has the highest affinity for EBI2 and the best solubility. We showed previously that unlabeled 7α,25-OHC (1 μM) did not displace binding significantly in mock-transfected COS-7 cells (Liu et al., 2011). Other available ligands have lower affinities for EBI2 and/or are much more hydrophobic. Use of those ligands at concentrations that saturated EBI2 binding often led to solubility problems. The reaction mixtures were incubated at room temperature for 1 h, filtered though a 96-well GFC filter plate, and washed three times with buffer (20 mM Tris-HCl, 10 mM $MgCl_2$, pH 7.4). Bound radioligand levels were assessed with the TopCount NXT counter, and the results were analyzed with GraphPad Prism 5. The maximal level of specific binding of [^{3}H]7α,25-OHC to wild-type EBI2 was expressed as 100% and was used for comparisons of radioligand binding to mutant receptors.

Molecular Modeling. Homology modeling of human EBI2 and subsequent docking of 7α,25-OHC were performed by using Discovery Studio 3.1 (Accelrys, San Diego, CA). The primary sequence alignment between the human β_2AR and EBI2 was determined by using the align123 program in Discovery Studio. The helical alignment was further examined and manually refined on the basis of multiple sequence alignments of family A GPCRs (Mirzadegan et al., 2003). The β_2AR structure (PDB code 2RH1) was used as a template for EBI2 except for TM2 and ECL2, for which CXCR4 (PDB code 3ODU) was used as a template. Each CXCR4 component was separately aligned with the β_2AR structure, to yield a hybrid β_2AR-CXCR4 template structure. On the basis of this hybrid template structure, an EBI2 homology model was built by using the homology modeling component of Discovery Studio.

The EBI2 homology model was placed in a 30-Å-thick implicit membrane and was energy-minimized by using the Smart Minimizer algorithm with the generalized Born with implicit membrane/implicit solvent model and the CHARMm force field. 7α,25-OHC was manually docked into the ligand binding site of the model EBI2 structure on the basis of GTPγS binding assay and radioligand binding assay data. After the ligand was docked into the binding site, a standard dynamics cascade (including steepest descent minimization, conjugate gradient minimization, heating of the system to 300°K, molecular dynamics equilibration, and production runs) was performed with the ligand constrained. The constraints on the ligand were then removed, and the entire system was further minimized to generate the final model of EBI2 with docked 7α,25-OHC.

Results

Effects of Ligand Structure on EBI2 Activation. [^{35}S]GTPγS binding assays were used for quantification of receptor activation. This type of assay measures the binding of nonhydrolyzable [^{35}S]GTPγS to the Gα subunit after agonist occupation of the receptor; it has the advantages of measuring one of the earliest receptor-mediated events in the signaling cascade and being less affected by downstream signaling amplification or modulation. We transfected COS-7 cells with EBI2 expression constructs in combination with G_{o2} protein because our previous studies showed that coexpression of G_{o2} increased ligand-stimulated [^{35}S]GTPγS incorporation and improved the signal/noise ratio (Liu et al., 2011).

Previously we showed that 7α,25-OHC activated EBI2 with high affinity and potency in recombinant systems (K_d = 450 pM; EC_{50} = 140 pM) (Liu et al., 2011). We also screened other oxysterols and cholesterol derivatives for their abilities to activate EBI2. We ranked, on the basis of ligand potency, the compounds that showed agonist activity, as follows: 7α,25-OHC (EC_{50} = 0.14 nM) > 7α,27-OHC (EC_{50} = 1.3 nM) > 7β,25-OHC (EC_{50} = 2.1 nM) > 7β,27-OHC (EC_{50} = 51 nM) > 7α-OHC (EC_{50} = 82 nM) > 25-OHC (EC_{50} = 127 nM) > 7β-OHC (EC_{50} = 1763 nM) > 27-OHC (EC_{50} = 3029 nM) (Liu et al., 2011). These findings strongly suggested that the hydroxyl groups in the 7′-, 25′-, or 27′-positions are important for EBI2 activation. It is important to note that cholesterol has a hydroxyl group in the 3′-position of the ring structure and this hydroxyl group was present in all of the oxysterols we tested previously. The importance of the 7′- and 25′-hydroxyl groups for EBI2 activation prompted us to ask whether the third hydroxyl group in 7α,25-OHC, in the 3′-position, also might play a role. To assess the functional significance of the 3′-hydroxyl group, we tested 7α,27-dihydroxy-4-cholesten-3-one, which is structurally similar to 7α,27-OHC except that its 3′-position has a ketone group instead of a hydroxyl group (Fig. 2A). Consistent with our previous report, 7α,27-OHC showed high potency in activating EBI2 (Fig. 2B; Table 1). In contrast, 7α,27-dihydroxy-4-cholesten-3-one at concentrations up to 10 μM showed little activity in stimulating [^{35}S]GTPγS incorporation by EBI2-expressing membranes (Fig. 2B; Table 1), which supports the hypothesis that the 3′-hydroxyl group is critical for maintaining agonist activity.

Biochemical Analysis of Receptor Expression Levels for Wild-Type and Mutant EBI2. To quantify receptor expression, we added a V5 tag to the N-terminal region of wild-type and mutant EBI2. In our previous study, we demonstrated that the N-terminal V5 tag did not affect EBI2 signaling (Liu et al., 2011). An anti-V5 antibody was used to label receptor proteins in transfected cells. Most mutant receptors showed similar total and cell-surface expression levels, compared with wild-type receptor levels, when protein levels were quantified with enzyme-linked immunosorbent assays (Supplemental Table 1). Three mutations, i.e., C104A (ECL1), C181A (ECL2), and F257A (TM6), resulted in ~50% reductions in total protein expression levels, compared with wild-type EBI2 levels (Table 2), which suggests that these three residues may be important for the biosynthesis or protein stability of EBI2. Several mutations, including C21A (N terminus), C104A (ECL1), C181A (ECL2), C280A (ECL3), P85A (TM2), Y90A (TM2), N114A (TM3), and F257A (TM6) (Table 2), resulted in substantial reductions in cell-surface receptor expression levels. These residues may be important for proper receptor folding, trafficking, and insertion into the cell membrane.

Investigation of Cysteine Residues in Extracellular Regions of EBI2. There are four Cys residues in the extracellular regions of EBI2, i.e., Cys21 (N terminus), Cys104 (ECL1), Cys181 (ECL2), and Cys280 (ECL3). We mutated these four Cys residues to Ala individually, to determine whether receptor expression, receptor function, and/or ligand binding was affected. The C104A and C181A mutations resulted in complete loss of cell-surface receptor expression but similar total receptor protein levels, compared with wild-type EBI2 values (Table 2), which suggests that Cys104 and Cys181 may be critical for proper EBI2 folding, trafficking, or insertion into the cell membrane. No signals were detected for these two mutants in GTPγS binding assays or radioligand binding assays (Fig. 3A; Table 2). Ala substitutions at Cys21 or Cys280 led to 70 to 80% reductions in cell-surface receptor expression levels and ~50% reductions in total protein expression levels (Table 2), which indicates additional roles in receptor biogenesis. In GTPγS binding assays, the C21A mutation in the N terminus caused a 20-fold increase in the EC_{50} of 7α,25-OHC and a ~75% decrease in E_{max}, compared with wild-type EBI2 values (Fig. 3A; Table 2). We did not detect any specific binding signals for the C21A mutant receptor, probably because of reduced ligand binding affinity and reduced cell-surface receptor expression. The C280A mutation in ECL3 resulted in relatively more-moderate reductions in receptor activity (EC_{50} = 0.93 nM for [^{35}S]GTPγS incorporation) (Fig. 3A) and radioligand binding (16.56% of the wild-type EBI2 value) (Table 2).

Mutations of Conserved Residues in Extracellular Regions of EBI2. The extracellular regions of GPCRs are highly variable but may contain important motifs for ligand

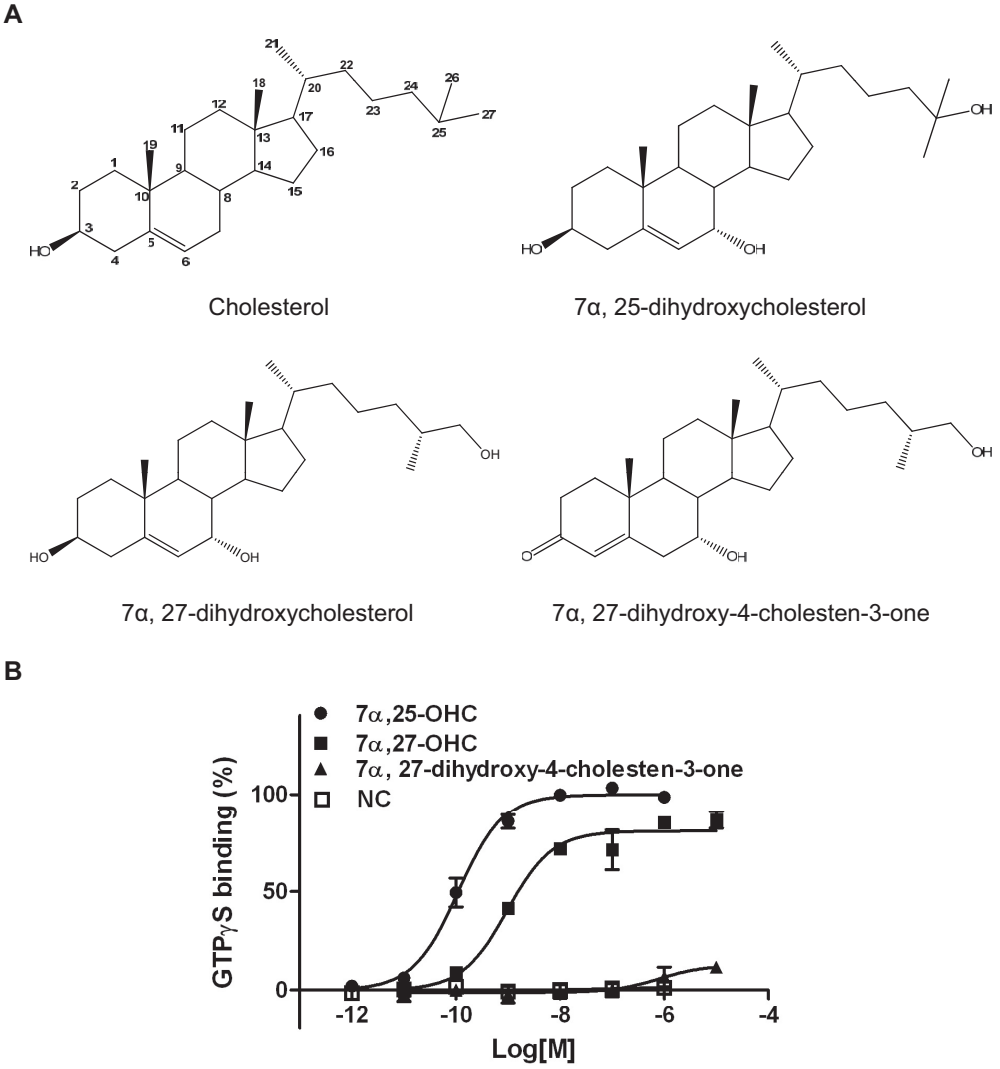

Fig. 2. Structure-activity studies with EBI2. A, structures of cholesterol, 7α,25-OHC, 7α,27-OHC, and 7α,27-dihydroxy-4-cholesten-3-one. B, comparison of EBI2 activation by 7α,25-OHC, 7α,27-OHC, and 7α,27-dihydroxy-4-cholesten-3-one in GTPγS binding assays. The assays were performed in triplicate, and values represent mean ± S.E.M. The results were analyzed with GraphPad Prism 5, and EC_{50} and E_{max} values are presented in Table 1. NC, negative control.

TABLE 1
Effects of ligand structure on EBI2 activation
The potency and efficacy of 7α,25-OHC, 7α,27-OHC, and 7α,27-dihydroxy-4-cholesten-3-one in activating EBI2 in [^{35}S]GTPγS binding assays were compared. EC_{50} values are the concentrations of compounds that stimulated 50% of the maximal response of wild-type EBI2. E_{max} values are expressed as percentages of the maximal response of wild-type EBI2 activated by 7α,25-OHC. The assays were performed in triplicate, and values represent mean ± S.E.M.

Ligand	EC_{50}	E_{max}
	nM	*% of wild-type response*
7α,25-OHC	0.11 ± 0.03	100
7α,27-OHC	0.97 ± 0.24	80.84 ± 4.62
7α,27-dihydroxy-4-cholesten-3-one	N.D.	N.D.

N.D., not determined, because the assay did not reach saturation.

binding and/or receptor activation. We compared human, rat, and mouse EBI2 sequences (Fig. 1A) and selected a number of conserved residues for mutagenesis studies (Fig. 1B). For example, the ECL2 contains a highly conserved region in positions 180 to 188, i.e., TCMEYPNFE. We made single Ala substitutions at these positions and characterized the mutant receptors pharmacologically. We also included in our study two single-nucleotide polymorphisms in the extracellular region, i.e., M93I (ECL1) and H284Y (ECL3), as listed in the National Institutes of Health National Center for Biotechnology Information single-nucleotide polymorphism database (www.ncbi.nlm.nih.gov/SNP/snp_ref.cgi?locusId=1880). Our results showed that most of the mutants had comparable levels of receptor expression and similar pharmacological profiles, compared with wild-type EBI2 (Table 2; Supplemental Table 1). In addition to Cys181, as mentioned above, we found that Ala substitution for Glu183 in ECL2 resulted in great reduction in the radioligand binding signal (11.33% of the wild-type value), although cell-surface expression was only moderately decreased (59.82% of the wild-type value) (Table 2). In agreement with the radioligand binding data, the E183A mutation resulted in an almost 50-fold reduction in ligand potency in GTPγS binding assays (Fig. 3B; Table 2).

Mutation Studies with Transmembrane Regions of EBI2. Transmembrane regions of GPCRs are highly conserved structurally, and the helical cores are thought to form the ligand binding pocket. On the basis of a method developed by Mirzadegan et al. (2003), we performed sequence alignments of EBI2 with GPCRs that have known crystal structures and well characterized ligand binding sites. Residues in EBI2 that were aligned at the sequence positions corresponding to the known ligand binding sites of GPCRs were selected for our mutation study (Fig. 1B).

TABLE 2

Characterization of selected EBI2 mutations

Recombinant EBI2 mutant receptors were characterized through receptor expression analyses, [^{35}S]GTPγS assays, and radioligand binding assay. Total expression and cell-surface expression were detected with an anti-V5 antibody in enzyme-linked immunosorbent assays, in the presence or absence of 1% Triton X-100 as the penetration reagent. The expression of N-terminally V5-tagged EBI2 is expressed as 100%. Cells without recombinant protein expression or with C-terminally V5-tagged GPR81 (GPR81-V5) were used as negative controls for protein expression. For the [^{35}S]GTPγS binding assays, EC_{50} values are the 7α,25-OHC concentrations that stimulated 50% of the maximal response for each individual mutant. E_{max} values are expressed as percentages of the maximal response of wild-type EBI2. The assays were performed in triplicate, and values represent mean ± S.E.M. For the radioligand binding assays, the total specific binding for each mutant was calculated as a percentage of the maximal specific [^{3}H]7α,25-OHC binding to wild-type EBI2.

Region of Residue Changed	Mutation	Receptor Expression		[^{35}S]GTPγS Binding		Specific Radioligand Binding
		Surface	Total	EC_{50}	E_{max}	
		% of WT level		*nM*	*% of WT response*	*% of WT level*
WT EBI2		100.00	100.00	0.11 ± 0.03	100	100.00
N terminus	C21A	20.68	59.97	2.29 ± 0.82	23.36 ± 1.21	5.42 ± 3.39
ECL1	C104A	2.75	90.22	N.A.	N.A.	N.A.
ECL2	C181A	5.49	79.51	N.A.	N.A.	N.A.
	E183A	59.82	74.26	5.46 ± 2.00	53.90 ± 2.07	11.33 ± 1.47
ECL3	C280A	32.60	53.24	0.93 ± 0.07	50.26 ± 2.00	16.56 ± 3.29
TM2	P85A	17.44	62.42	2.16 ± 1.67	27.28 ± 8.37	6.37 ± 1.43
	Y90A	23.56	80.78	23.74 ± 3.25	39.74 ± 1.81	N.A.
	D77A	86.97	78.50	N.A.	N.A.	99.31 ± 5.86
	R87A	110.84	117.04	49.04 ± 7.72	49.97 ± 1.01	N.A.
	R87W	77.13	144.55	64.01 ± 4.01	76.17 ± 0.86	17.59 ± 8.72
	R87K	75.63	78.64	3.99 ± 0.36	78.21 ± 1.43	78.02 ± 9.35
TM3	N114A	47.63	77.51	N.A.	N.A.	15.98 ± 5.04
	Y112A	91.83	89.34	11.42 ± 2.49	96.01 ± 3.22	9.39 ± 4.04
	Y116A	118.08	110.49	9.13 ± 0.92	51.71 ± 4.99	N.A.
TM5	L197A	105.57	116.52	11.78 ± 0.76	87.93 ± 3.36	20.21 ± 1.77
TM6	F257A	35.86	45.06	0.11 ± 0.21	36.74 ± 3.43	15.85 ± 2.26
	Y260A	114.07	125.93	140.50 ± 6.87	125.90 ± 2.15	N.A.
	H261A	79.95	97.96	63.71 ± 17.19	44.81 ± 3.68	4.65 ± 1.54
	I264A	112.03	104.26	1.72 ± 0.49	73.30 ± 7.87	10.84 ± 3.48
TM7	V294A	74.29	137.79	3.11 ± 4.60	80.37 ± 4.42	47.65 ± 2.24
	M297I	105.34	90.98	4.09 ± 0.42	92.88 ± 2.09	36.95 ± 3.71
	M297A	110.75	142.23	0.68 ± 0.04	158.5 ± 4.63	93.55 ± 5.05

WT, wild-type; N.A., not applicable, because no receptor stimulation by 7α,25-OHC or specific binding was observed.

As noted above, the P85A (TM2), Y90A (TM2), N114A (TM3), and F257A (TM6) mutations resulted in ≥50% reductions in cell-surface receptor expression levels. Although the N114A mutant still exhibited a 50% cell-surface expression level, its maximal radioligand binding level was only ~15.98%, compared with the wild-type values. Moreover, this mutant receptor was nonfunctional, because no GTPγS binding could be detected even with 1 μM 7α,25-OHC (Fig. 3D; Table 2).

We also found a series of mutations in the transmembrane regions that did not affect cell-surface receptor expression levels but had negative effects on receptor activity in GTPγS assays (Fig. 3; Table 2). To understand whether the functional disruption was attributable to the inability to bind 7α,25-OHC, we tested these mutants in radioligand binding assays. For comparison of ligand binding levels, we were able to perform only competitive radioligand binding assays, rather than saturation binding assays, because of the limited stock of [^{3}H]7α,25-OHC available and the large collection of mutants we generated. We confirmed that almost all of the mutants exhibited reduced or abolished [^{3}H]7α,25-OHC binding. For example, when Arg87 in TM2 was mutated to Ala or Trp, radioligand binding was greatly decreased (3% or 17.59% of the wild-type value, respectively). Consequently, the ligand potency in GTPγS binding assays was reduced 449- or 582-fold, respectively. Mutation of Arg87 to Lys, another amino acid with a positively charged side chain, did not have any significant effect on receptor activity or ligand binding. Arg87 has been reported to be important for the constitutive activity of EBI2, and we did not assess the constitutive activity of EBI2 in this study. However, our result suggests that Arg87 is important for ligand activation of EBI2. Other transmembrane region residues that showed reduced ligand binding and receptor function after Ala mutation included Tyr112 and Tyr116 of TM3, Leu197 of TM5, Tyr260, His261, and Ile264 of TM6, and Val294 and Met297 of TM7 (Table 2).

Importance of Asp77 in TM2 for Receptor Activation. The majority of mutations that negatively affected receptor activation were found to be important also for ligand binding. Receptors with the single amino acid change of Asp77 in TM2 to Ala retained normal ligand binding (Table 2). Asp77 is not involved in receptor biogenesis or trafficking, inasmuch as both cell-surface and total protein expression levels were similar to wild-type EBI2 levels (Table 2). However, this mutant receptor showed no [^{35}S]GTPγS incorporation even with 1 μM 7α,25-OHC (Fig. 3E; Table 2). Such a pharmacological profile suggests that Asp77 is not involved in ligand binding but might be important for receptor activation or signal transduction. The aspartic acid in TM2 is a highly conserved residue among family A GPCRs. In the available GPCR crystal structures, this aspartic acid lies below the ligand binding site in what is considered a water channel, and it is important for transmission of the signal upon ligand binding to the G-protein binding site on the intracellular side of the GPCR (Angel et al., 2009).

Homology Modeling of Human EBI2 and Ligand Docking. The β_2AR structure (PDB code 2RH1) (Cherezov et al., 2007) has 52.9% sequence similarity to EBI2 in the transmembrane regions. Therefore, it was used as a template for building of the homology model. During manual refinement after multiple sequence alignments with family A GPCRs

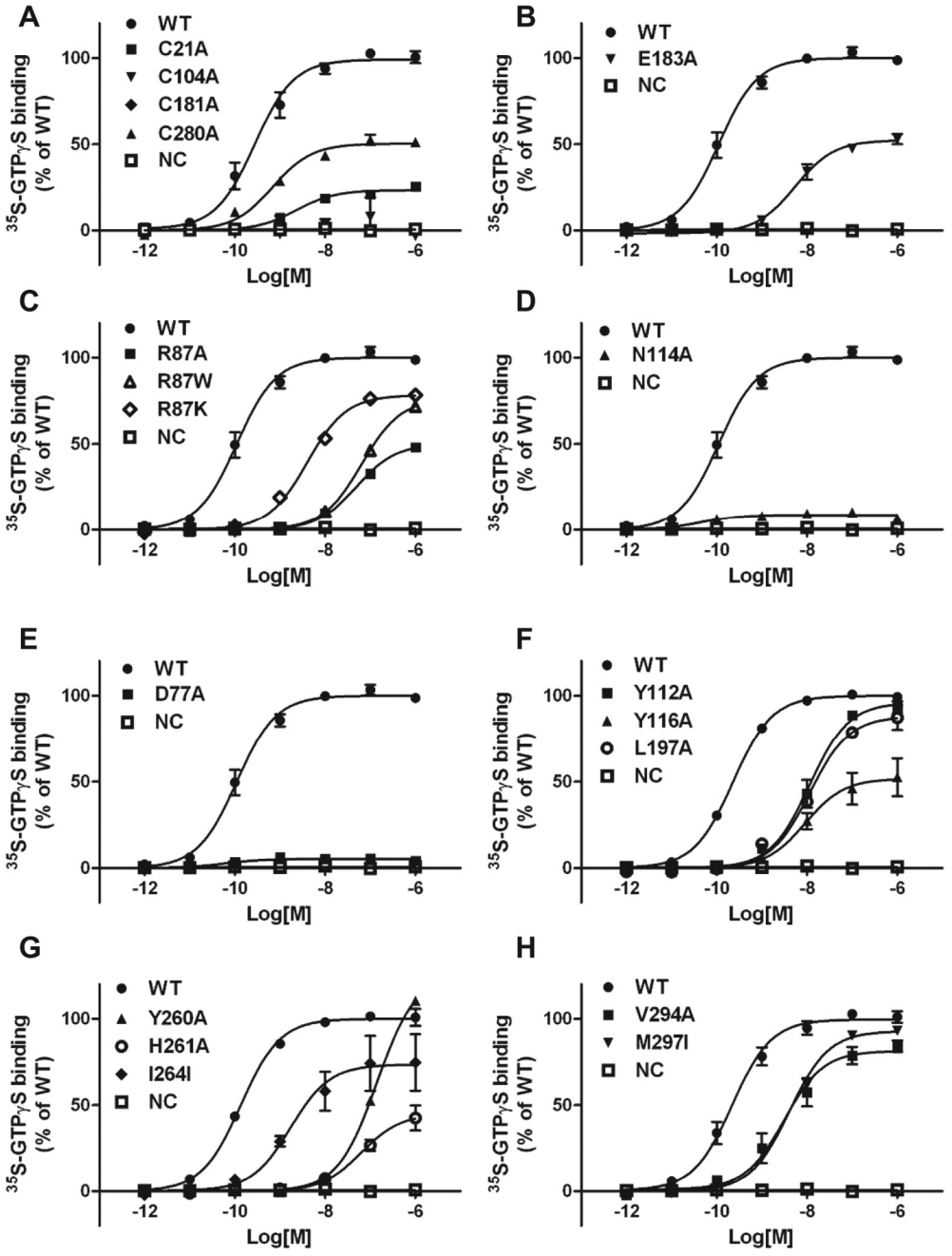

Fig. 3. Pharmacological characterization of selected EBI2 mutants in [^{35}S]GTPγS binding assays. Ligand-stimulated [^{35}S]GTPγS incorporation levels were normalized to basal [^{35}S]GTPγS incorporation in the absence of ligand and are expressed as percentages of the maximal response of wild-type EBI2. The assays were performed in triplicate, and values represent mean ± S.E.M. The results were analyzed with GraphPad Prism 5, and EC_{50} and E_{max} values are presented in Table 2. Membranes from cells expressing wild-type (WT) human EBI2 and cells transfected with only G_{o2} were used as the positive control and negative control (NC), respectively.

(Mirzadegan et al., 2003), we found that TM2 of EBI2 exhibits structural features similar to those of CXCR4 (PDB code 3ODU) because of the proline residue in this region (Pro85 in EBI2 and Pro92 in CXCR4) (Fig. 4A). In addition, ECL2 of EBI2 exhibits greater sequence similarity to CXCR4 (35%) than to β_2AR (24%) (Fig. 4B). Therefore, CXCR4 was used as the template structure for the TM2 and ECL2 regions of EBI2. For modeling of the ligand binding site, 7α,25-OHC was manually docked on the basis of results from our structure-activity studies. The three hydroxyl groups (in the 3′-, 7′-, and 25′-positions) of 7α,25-OHC were determined to be essential for receptor-ligand interactions and were used to orient the ligand. The final model of EBI2 with 7α,25-OHC docked is shown in Fig. 4, C and D. As illustrated in our proposed model, Arg87 of EBI2 interacts with the 7α′-hydroxyl group of 7α,25-OHC, Asn114 interacts with the 25′-hydroxyl group, and Glu183 interacts with the 3′-hydroxyl group. Asp77 lies just below the modeled ligand binding site and likely plays a role in signal transmission and receptor activation. Residues Tyr112, Tyr116, Leu197, His261, Val294, and Met297 form hydrophobic interactions with the steroidal body of 7α,25-OHC.

Discussion

Importance of 7α,25-OHC Hydroxyl Groups for Receptor Activation. The identification of 7α,25-OHC as the endogenous ligand for EBI2 provides a pharmacological tool for activation of the receptor in vitro and investigation of the molecular mechanisms underlying EBI2 activation (Hannedouche et al., 2011; Liu et al., 2011). Here we used a mutagenesis approach to identify the residues in EBI2 that are

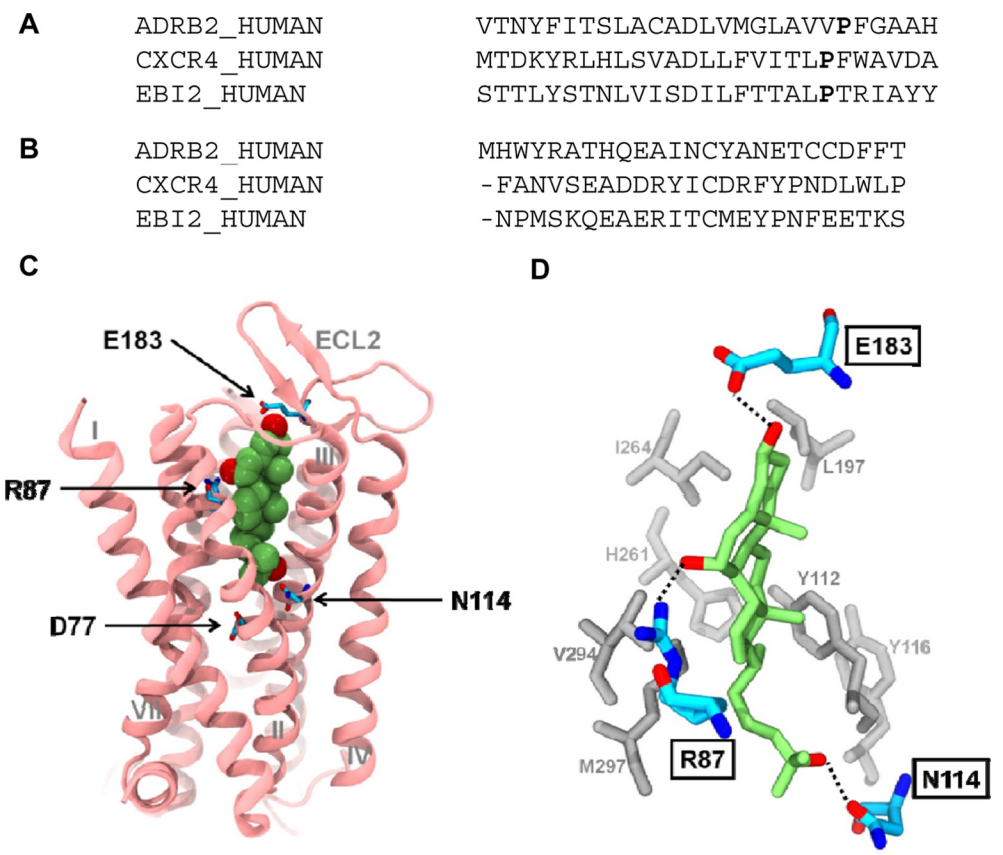

Fig. 4. A, sequence alignment of EBI2 transmembrane helix 2 with those of β_2AR and CXCR4. CXCR4 was chosen as the template for the modeling of EBI2 helix 2 because of the position of the proline at position 21, compared with position 22 in the β_2AR. B, sequence alignment of EBI2 extracellular loop 2 with those of β_2AR and CXCR4. C, homology model of EBI2 with docked 7α,25-OHC. The homology model was created by using CXCR4 (PDB code 3ODU) as a template for helix 2 and ECL2. Each of the CXCR4 segments was separately aligned with the β_2AR (PDB code 2RH1), which was used as a template for the remaining helices and loops. 7α,25-OHC was manually docked in the EBI2 homology model by using available structure-activity relationship data. The hydroxyl groups of 7α,25-OHC interact with residues Arg87, Asn114, and Glu183 on EBI2. Residue Asn77 is not involved in ligand binding but is highly conserved and is important for transmission of the GPCR signal. The disulfide bond formed by Cys104 and Cys181 is structurally important in maintaining the position of the ECL2 loop, which partially caps the ligand binding site, and the positioning of Glu183. D, close-up view of the ligand binding site of EBI2. 7α,25-OHC is oriented in the binding site of EBI2 with the 25′-hydroxyl group interacting with the Asn144 carboxamide group, the 7α′-hydroxyl group interacting with the Arg87 guanidinium group, and the 3′-hydroxyl group (native to cholesterol) interacting with the Glu183 carboxylate group. The remaining residues, i.e., Tyr112, Tyr116, Leu197, His261, Val294, and Met297, form hydrophobic interactions with the steroidal body of 7α,25-OHC.

critical for receptor function or ligand binding. We previously tested more than 40 oxysterols and cholesterol derivatives with EBI2 and validated 7α,25-OHC as the most potent ligand. We also were able to extrapolate structure-activity correlations from these results, to help elucidate the key molecular drivers involved in ligand activation. Oxysterols are oxygenated derivatives of cholesterol. Although cholesterol was completely inactive with EBI2, the addition of a hydroxyl group to the steroidal ring structure (as in 7α-OHC and 7β-OHC) or to the hydrocarbon tail (as in 25-OHC or 27-OHC) was able to confer agonist activity, with EC_{50} values ranging from 100 nM to low micromolar levels (Hannedouche et al., 2011; Liu et al., 2011). Dihydroxycholesterols with two additional hydroxyl groups, compared with cholesterol (e.g., 7α,25-OHC, 7β,25-OHC, 7α,27-OHC, and 7β,27-OHC), were found to activate EBI2 with much greater potency. The position of the hydroxyl group is also a critical determinant. To our knowledge, addition of a hydroxyl group to the 4′-, 5′-, 6′-, 15′-, 22′-, or 24′-position was unable to induce any agonist activity (Liu et al., 2011). It is possible that only the 7′-, 25′-, and 27′-positions allow the hydroxyl groups to adopt the correct conformations for contacting key residues in the ligand binding site and forming optimal hydrogen bond interactions. The rank order of active oxysterols on the basis of functional potency (7α,25-OHC > 7α,27-OHC > 7β,25-OHC > 7β,27-OHC > 7α-OHC > 25-OHC > 7β-OHC > 27-OHC) correlates well with their binding affinities. It is reasonable to postulate that, to achieve the optimal interactions between the receptor and ligands, a hydroxyl group in the 7α′-position has a more-favorable conformation than one in the 7β′-position and a second hydroxyl group in the 25′-position is more favorable than one in the 27′-position.

The 3′-hydroxyl group is native to cholesterol and is present in all of the other oxysterols we tested. Although 7α,27-OHC was the second most potent agonist for EBI2, the substitution of the 3′-hydroxyl group with a ketone group abolished the ability to activate EBI2. Taken together, these findings indicate that all three hydroxyl groups (3′, 7α′, and 25′) in 7α,25-OHC are involved in ligand binding and receptor activation, and the positions and orientations of the hydroxyl groups play key roles in determining agonist activity.

Evidence that Glu183 in ECL2 Is Held by Classic Disulfide Bridge and Caps Ligand Binding Site. Certain structural features are conserved among almost all members

of the GPCR superfamily, one of which is a disulfide bridge formed between a conserved Cys residue in ECL2 and another conserved Cys residue in ECL1 near the top of TM3 (Gether 2000; Karnik et al., 2003). This covalent linkage, which is present in >90% of all GPCRs, is acknowledged to be important for the tertiary integrity of GPCRs, ligand gating, and even ligand binding (Klco et al., 2005). Our data suggest that Cys104 and Cys181 are functionally more equivalent, whereas Cys21 is more similar to Cys280, which supports our hypothesis that Cys104 (ECL1) and Cys181 (ECL2) form the classic disulfide bond, whereas Cys21 (N terminus) and Cys280 (ECL3) may form a second disulfide bridge. This pattern of extracellular disulfide bridges is the same as in CXCR4, which also has four extracellular Cys residues distributed in the N terminus, ECL1, ECL2, and ECL3. The crystal structure of CXCR4 confirmed the two disulfide bridges, i.e., Cys109-Cys186 linking ECL2 with the extracellular end of TM3 and Cys28-Cys274 connecting the N terminus to the extracellular tip of TM7 (Wu et al., 2010).

This proposed model of two disulfide bridges has important functional implications. Because of the Cys104-Cys181 link, ECL2 is brought close to the transmembrane domain and may form a cap over the putative ligand binding site (Fig. 4C), similar to findings observed for most GPCRs. ECL2 thus may be positioned to interact with the ligand. Glu183, which is just two residues from Cys181, is the best candidate for forming a hydrogen bond with one of the hydroxyl groups of 7α,25-OHC. Our mutagenesis data confirmed that Ala substitution at Glu183 disrupted ligand binding and receptor activity (Fig. 3B; Table 2), which supports our hypothesis that Glu183 is held by the disulfide bridge over the ligand binding pocket so that the hydroxyl group of 7α,25-OHC can interact with the Glu183 carboxylate group. The inactivity of 7α,27-dihydroxy-4-cholesten-3-one provided more evidence that the 3′-hydroxyl group interacts with Glu183, because a ketone interacting with the carboxylate would be energetically unfavorable. Taken together, the results suggest an important structural role for ECL2 in ligand activation of EBI2.

Molecular Modeling of Ligand Binding Pocket of EBI2. EBI2 is the first GPCR known to bind an oxysterol as an endogenous ligand (Hannedouche et al., 2011; Liu et al., 2011). Therefore, it is of particular interest to understand how 7α,25-OHC interacts with EBI2 and which molecular determinants are critical for this interaction. The β_2AR structure (PDB code 2RH1) has 52.9% sequence similarity to EBI2 in the transmembrane regions and was used as a template for building the EBI2 homology model. For EBI2 TM2, however, CXCR4 TM2 was chosen over the β_2AR as a template, because Pro85 in EBI2 TM2 aligns with Pro92 in CXCR4 TM2, whereas the proline in the β_2AR (Pro88) is shifted by one residue (Fig. 4A). Proline residues break helical secondary structures, which produces a kink in the helix. Shifting a proline residue by even a single position would cause the remaining helix to be kinked in a slightly different orientation. Arg87, which lies two residues above Pro85, was crucial for ligand binding. Therefore, we used CXCR4 TM2 as a template to ensure that the helix would be kinked in the correct position and the remaining downstream residues, including Arg87, would be in the proper orientation. The crystal structures of GPCRs show very different ECL2 structures. ECL2 of CXCR4 was chosen as the template for EBI2 because it has similar length and greater sequence similarity (35%) with respect to EBI2, among the available GPCRs with known crystal structures (Fig. 4B). This created a hybrid structure in which the β_2AR was used as the base structure, whereas TM2 was kinked and ECL2 was modeled as in CXCR4. The use of a hybrid template for GPCR homology modeling was reported previously (Worth et al., 2009, 2011).

After the EBI2 homology model based on the hybrid β_2AR-CXCR4 template was built, 7α,25-OHC was manually docked into the ligand binding site. Of all residues that were identified as being important for ligand binding, Arg87, Asn114, and Glu183 are polar or charged residues that might interact with the three hydroxyl groups in 7α,25-OHC. As expected, alanine mutations for Arg87, Asn114, and Glu183 led to functional disruption and were subsequently used to orient the ligand and to optimize the EBI2 homology model (Fig. 4). In the final docked model, 7α,25-OHC is oriented with the 25′-hydroxyl group interacting with the Asn144 carboxamide group, the 7α′-hydroxyl group interacting with the Arg87 guanidinium group, and the 3′-hydroxyl group (native to cholesterol) interacting with the Glu183 carboxylate group (Fig. 4, C and D). The orientation of Arg87 with the 7α′-hydroxyl group is consistent with the observation that 7α,25-OHC is more potent than 7β,25-OHC in activating EBI2. Because the steroidal body of 7α,25-OHC is rigid, a hydroxyl group in the 7β′-conformation would be constrained, which would hinder optimal contact with the guanidinium group in Arg87. It was reported previously that Arg87 might act as a positive regulator for the constitutive activity of EBI2, because substitution of Arg87 with Ala but not Lys significantly reduced constitutive activity (Benned-Jensen and Rosenkilde, 2008). This is in line with our finding that the R87A mutation but not the R87K mutation resulted in reduced ligand activation, which suggests that Arg87 may serve as an important molecular switch between the inactive and active states of EBI2.

The interaction between Asn114 and the 25′-hydroxyl group provides the structural basis for the better potency of 7α,25-OHC, compared with 7α,27-OHC, because the hydroxyl group at the 27′-position would not reach as close to Asn114 for optimal interactions. Other evidence supporting the putative orientation of 7α,25-OHC includes the observation that the M297I mutation but not the M297A mutation decreased ligand binding. In the docked homology model, M297 lies tight against the steroidal body of 7α,25-OHC. A more-bulky, branched-chain amino acid such as Ile at this position would have unfavorable steric interactions with the rigid steroidal ring structure of the ligand.

In conclusion, our results suggest that all three hydroxyl groups (3′, 7α′, and 25′) of the ligand are important for receptor binding and activation, with the 3′-hydroxyl group interacting with Glu183, the 7α′-hydroxyl group interacting with Arg87, and the 25′-hydroxyl group interacting with Asn114. The proposed EBI2 homology model described in this report includes the critical chemical and structural features of the binding pocket and may be useful for future, structure-based, drug-discovery efforts.

Authorship Contributions

Participated in research design: Zhang, Shih, Yang, Wu, Mirzadegan, Sun, Lovenberg, and Liu.

Conducted experiments: Zhang, Shih, Yang, Kuei, and Liu.

Contributed new reagents or analytic tools: Wu, Deng, and Mani.

Performed data analysis: Zhang, Shih, Yang, Kuei, Mirzadegan, and Liu.

Wrote or contributed to the writing of the manuscript: Zhang, Shih, Yang, Mirzadegan, Sun, Lovenberg, and Liu.

References

Angel TE, Chance MR, and Palczewski K (2009) Conserved waters mediate structural and functional activation of family A (rhodopsin-like) G protein-coupled receptors. *Proc Natl Acad Sci USA* **106:**8555–8560.

Benned-Jensen T and Rosenkilde MM (2008) Structural motifs of importance for the constitutive activity of the orphan 7TM receptor EBI2: analysis of receptor activation in the absence of an agonist. *Mol Pharmacol* **74:**1008–1021.

Benned-Jensen T, Smethurst C, Holst PJ, Page KR, Sauls H, Sivertsen B, Schwartz TW, Blanchard A, Jepras R, and Rosenkilde MM (2011) Ligand modulation of the Epstein-Barr virus-induced seven-transmembrane receptor EBI2: identification of a potent and efficacious inverse agonist. *J Biol Chem* **286:**29292–29302.

Birkenbach M, Josefsen K, Yalamanchili R, Lenoir G, and Kieff E (1993) Epstein-Barr virus-induced genes: first lymphocyte-specific G protein-coupled peptide receptors. *J Virol* **67:**2209–2220.

Cherezov V, Rosenbaum DM, Hanson MA, Rasmussen SG, Thian FS, Kobilka TS, Choi HJ, Kuhn P, Weis WI, Kobilka BK, et al. (2007) High-resolution crystal structure of an engineered human β_2-adrenergic G protein–coupled receptor. *Science* **318:**1258–1265.

Gatto D, Paus D, Basten A, Mackay CR, and Brink R (2009) Guidance of B cells by the orphan G protein-coupled receptor EBI2 shapes humoral immune responses. *Immunity* **31:**259–269.

Gatto D, Wood K, and Brink R (2011) EBI2 operates independently of but in cooperation with CXCR5 and CCR7 to direct B cell migration and organization in follicles and the germinal center. *J Immunol* **187:**4621–4628.

Gether U (2000) Uncovering molecular mechanisms involved in activation of G protein-coupled receptors. *Endocr Rev* **21:**90–113.

Hannedouche S, Zhang J, Yi T, Shen W, Nguyen D, Pereira JP, Guerini D, Baumgarten BU, Roggo S, Wen B, et al. (2011) Oxysterols direct immune cell migration via EBI2. *Nature* **475:**524–527.

Karnik SS, Gogonea C, Patil S, Saad Y, and Takezako T (2003) Activation of G-protein-coupled receptors: a common molecular mechanism. *Trends Endocrinol Metab* **14:**431–437.

Kelly LM, Pereira JP, Yi T, Xu Y, and Cyster JG (2011) EBI2 guides serial movements of activated B cells and ligand activity is detectable in lymphoid and nonlymphoid tissues. *J Immunol* **187:**3026–3032.

Klco JM, Wiegand CB, Narzinski K, and Baranski TJ (2005) Essential role for the second extracellular loop in C5a receptor activation. *Nat Struct Mol Biol* **12:**320–326.

Liu C, Eriste E, Sutton S, Chen J, Roland B, Kuei C, Farmer N, Jörnvall H, Sillard R, and Lovenberg TW (2003) Identification of relaxin-3/INSL7 as an endogenous ligand for the orphan G-protein-coupled receptor GPCR135. *J Biol Chem* **278:**50754–50764.

Liu C, Wilson SJ, Kuei C, and Lovenberg TW (2001) Comparison of human, mouse, rat, and guinea pig histamine H4 receptors reveals substantial pharmacological species variation. *J Pharmacol Exp Ther* **299:**121–130.

Liu C, Yang XV, Wu J, Kuei C, Mani NS, Zhang L, Yu J, Sutton SW, Qin N, Banie H, et al. (2011) Oxysterols direct B-cell migration through EBI2. *Nature* **475:**519–523.

Mirzadegan T, Benkö G, Filipek S, and Palczewski K (2003) Sequence analyses of G-protein-coupled receptors: similarities to rhodopsin. *Biochemistry* **42:**2759–2767.

Pereira JP, Kelly LM, and Cyster JG (2010) Finding the right niche: B-cell migration in the early phases of T-dependent antibody responses. *Int Immunol* **22:**413–419.

Pereira JP, Kelly LM, Xu Y, and Cyster JG (2009) EBI2 mediates B cell segregation between the outer and centre follicle. *Nature* **460:**1122–1126.

Rose KA, Stapleton G, Dott K, Kieny MP, Best R, Schwarz M, Russell DW, Björkhem I, Seckl J, and Lathe R (1997) Cyp7b, a novel brain cytochrome P450, catalyzes the synthesis of neurosteroids 7α-hydroxy dehydroepiandrosterone and 7α-hydroxy pregnenolone. *Proc Natl Acad Sci USA* **94:**4925–4930.

Rosenkilde MM, Benned-Jensen T, Andersen H, Holst PJ, Kledal TN, Lüttichau HR, Larsen JK, Christensen JP, and Schwartz TW (2006) Molecular pharmacological phenotyping of EBI2: an orphan seven-transmembrane receptor with constitutive activity. *J Biol Chem* **281:**13199–13208.

Vassilatis DK, Hohmann JG, Zeng H, Li F, Ranchalis JE, Mortrud MT, Brown A, Rodriguez SS, Weller JR, Wright AC, et al. (2003) The G protein-coupled receptor repertoires of human and mouse. *Proc Natl Acad Sci USA* **100:**4903–4908.

Worth CL, Kleinau G, and Krause G (2009) Comparative sequence and structural analyses of G-protein-coupled receptor crystal structures and implications for molecular models. *PLoS One* **4:**e7011.

Worth CL, Kreuchwig A, Kleinau G, and Krause G (2011) GPCR-SSFE: a comprehensive database of G-protein-coupled receptor template predictions and homology models. *BMC Bioinformatics* **12:**185.

Wu B, Chien EY, Mol CD, Fenalti G, Liu W, Katritch V, Abagyan R, Brooun A, Wells P, Bi FC, et al. (2010) Structures of the CXCR4 chemokine GPCR with small-molecule and cyclic peptide antagonists. *Science* **330:**1066–1071.

Address correspondence to: Changlu Liu, Janssen Pharmaceutical Research and Development, 3210 Merryfield Row, San Diego, CA 92121. E-mail: cliu9@its.jnj.com